ACS APPLIED MATERIALS & INTERFACES

Research Article

www.acsami.org

Fast Responsive and Highly Efficient Optical Upconverter Based on Phosphorescent OLED

Xinbo Chu,[†] Min Guan,*[,†] Litao Niu,[†] Yiping Zeng,[†] Yiyang Li,[†] Yang Zhang,*[,†] Zhanping Zhu,[†] and Baoqiang Wang[†]

[†]Key Laboratory of Semiconductor Materials Science, Institute of semiconductors, Chinese Academy of Sciences, Beijing, China

Supporting Information

ABSTRACT: In this work, an organic−inorganic hybrid optical upconverter that can convert irradiated 980 nm IR light to 510 nm green phosphorescence sensitively was fabricated and studied. *fac*-Tris(2-phenylpyridine) iridium ($Ir(ppy)_3$) doped 4,4′-bis(*N*-carbazolyl)-1,1′-biphenyl (CBP) was used as emitting layer in the phosphorescent organic light-emitting diode (OLED) unit. The upconverter using a phosphorescent OLED as display unit can achieve a higher upconversion efficiency and a low power consumption when compared with the one using fluorescent. An upconversion efficiency of 4.8% can be achieved for phosphorescent device at 15 V, much higher than that of fluorescent one (2.0%). The upconverter's transient optical and electric response to IR pulse were also investigated for the first time. The response time was found to be influenced by IR intensity and applied voltage. It has a response time as short as 60 μs. The rapid response property of the upconverter makes it feasible to be applied to high-speed IR imaging systems.

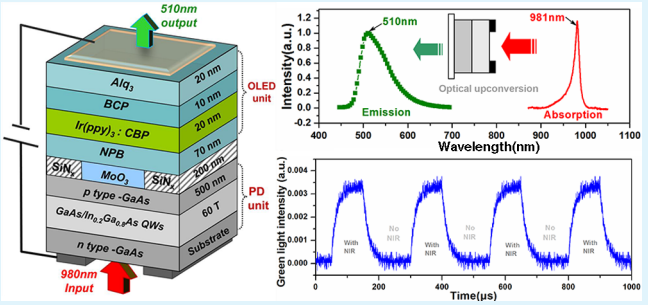

KEYWORDS: *OLED, infrared photo detector, optical upconverter, organic−inorganic hybrid device, phosphorescent, fast response*

42.79.Pw, 85.60.Bt, 85.60.Jb

INTRODUCTION

Infrared imaging devices have been receiving widespread interest in view of their potential applications in night vision, national defense, and biomedical research.[1−3] The present IR imaging is commonly achieved by interconnecting IR focal plane detector arrays with readout circuit via indium bump technology.[4,5] However, this hybridization process is both time-consuming and costly. To better solve this problem, the optical upconversion technology has been proposed and researched for years as an alternative method.[6−10] Overall, the upconverters that can convert inputted long-wavelength IR to visible light are fabricated by tandem integration of a photodetector (PD) unit with a display unit.

Depending on different material systems employed in the two units, the upconverter can be classified into three types: all inorganic material-based,[11−13] all organic material-based[14−16] and the hybrid one that combined an inorganic PD with OLED.[17−21] As the "lattice-matching" requirement for organic material is far less stringent than that of inorganic semiconductors, organic layer can be deposited easily and cheaply on any substrate.[22] In addition, the emission wavelength of OLED can be tuned across visible region easily.[23−25] Therefore, this hybrid method is able to suitably combine the superiority of both material systems and complement each other's advantages.[26−29] Even though the inorganic PD units possess a high responsivity, the low conversion efficiency is still the obstacle to the development of an organic−inorganic (OI) hybrid upconverter.

In this thesis, considering the high quantum efficiency of phosphorescent material, the upconverter adopting phosphorescent OLED as display unit was fabricated to improve the overall upconversion efficiency. It shows a superior performance than the fluorescent one, which had been studied in our former work.[30,31] Furthermore, the response property must be considered if the OI hybrid upconverter was applied to IR imaging for 1 d.[32,33,34] Therefore, the transient response test system was designed and set up for the first time to investigate the optical and electric response. The understanding of these processes may give a better insight into the kinetics of carriers and excitons. It is shown that the response time was influenced by IR intensity and applied voltage. A response time as short as 60 μs can be obtained, indicating that it has a great application potential in high-speed IR imaging field.

EXPERIMENTAL SECTION

Preparation of the Near-Infrared Photodetector Unit. The GaAs-based IR PD unit was fabricated in VEECO GEN-II molecular beam epitaxial (MBE) system. It was composed of 60 pairs of $In_{0.2}Ga_{0.8}As$/GaAs multiquantum wells (MQWs), which were

Received: July 25, 2014
Accepted: October 13, 2014
Published: October 13, 2014

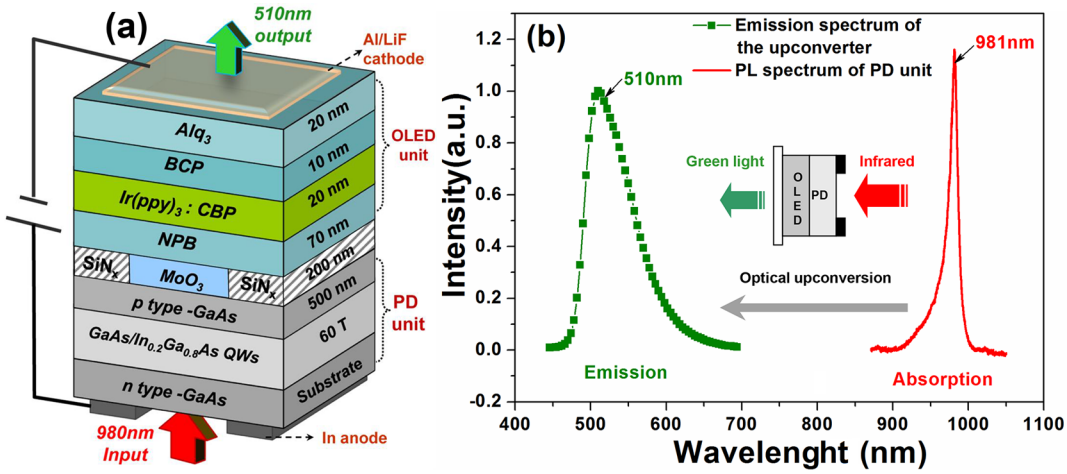

Figure 1. (a) The cross-section schematic of the organic–inorganic hybrid upconverter. (b) Photoluminescence (PL) spectrum of the PD unit and emission spectrum of the upconverter in working state.

sandwiched between 300 nm n^+-GaAs (3×10^{18} cm^{-3}, bottom) and 500 nm p^+-GaAs (5×10^{18} cm^{-3}, top) layer as IR absorption layer. Figure 1a shows the cross-section schematic diagram of the organic–inorganic hybrid upconverter. The p-type GaAs top layer also acted as an anode contact in OLED unit. 200 nm SiN_x film was deposited on top of p-type GaAs surface as electrical isolation layer. Then 1 mm × 1 mm square windows were patterned using standard photolithography and etched onto the SiN_x layer using dry etching. Metal In was deposited on the back of the PD unit, serving as the bottom contact for the upconverter.

Fabrication of the OLED Unit. The PD unit was boiled for 5 min in a mixture of sulfuric acid and phosphoric acid (H_2SO_4/H_3PO_4 = 3:1) to remove surface oxides and was then ultrasonically cleaned, first in ethanol and then in acetone, in each case for 5 min. Then, the sample was transferred into an organic molecular beam deposition system (OMBD) with a vacuum of 2.0×10^{-8} Torr for OLED layers deposition. Five nanometer MoO_3 was inserted between p-GaAs and *N*,*N*′-diphenyl-*N*,*N*′-bis(1,1′-biphenyl)-4,4′- diamine (NPB) as an interfacial layer to promote the photocarrier injection from PD to OLED unit. NPB, tris(8-hydroxyquinoline)aluminum (Alq_3) and 2,9-dimethyl-4,7-diphenyl-1,10-phenanthroline (BCP) were used as hole-transporting layer (HTL), electron-transporting layer (ETL), and hole-blocking layer (HBL), respectively. The upconverter using *fac*-tris(2-phenylpyridine) iridium doped 4,4′-bis(*N*-carbazolyl)-1,1′-biphenyl [$Ir(ppy)_3$:CBP] as emitting layer (EML) was named as Phosphorescent Device. The molar concentration of $Ir(ppy)_3$ in EML was 9%. As a comparison, the device using 10-(2-benzo-thiazolyl)-2,3,6,7-tetrahydro-1,1,7,7-tetramethyl-1*H*,5*H*,11*H*-(1)-benzopyropyrano(6,7,8-*i*,*j*) quinolizin-11-one (C545T):Alq_3 as EML was named as Fluorescent Device. LiF (1 nm)/Al (20 nm) semitransparent cathode was deposited on top of the organic stack finally. The emission area of the devices was 1 mm^2 determined by the overlap area of GaAs square windows and cathode.

Optoelectrical Characterization. The current density–voltage-luminescence (J-V-L) characteristics were measured by a Keithley electrometer 2400 and a ST-86LA spot photometer. The emission spectra of the upconverter were obtained by using a PR-650 Spectra Colorimeter. The response property test system was designed and set up for the first time. As shown in Figure 5, it was composed of an IR laser driven by a step pulse generator (PCX-7420), a fast photomultiplier tube (PMT), and a fast digital oscilloscope (RIGOL DS1062CA). All measurements were carried out under ambient conditions without any protective coating.

RESULT AND DISCUSSIONS

Figure 1a displays the structure diagram and working mechanism of the OI hybrid upconverter. It was mainly composed of two components, namely, the PD unit and the OLED unit. In the PD unit, 60 period undoped $In_{0.2}Ga_{0.8}As$/GaAs quantum wells (QWs) was inserted between n-GaAs and p-GaAs layers as IR absorption layer. The upconverter using $Ir(ppy)_3$:CBP as EML was named as Phosphorescent Device.

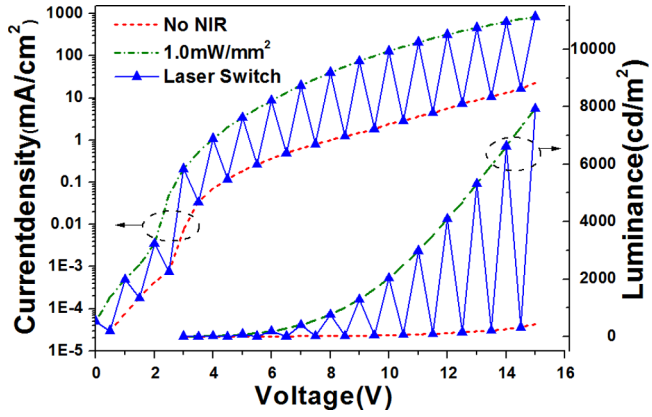

Figure 2. Output brightness and current density with and without laser irradiance at different bias. The IR power density was 1 mW/mm^2.

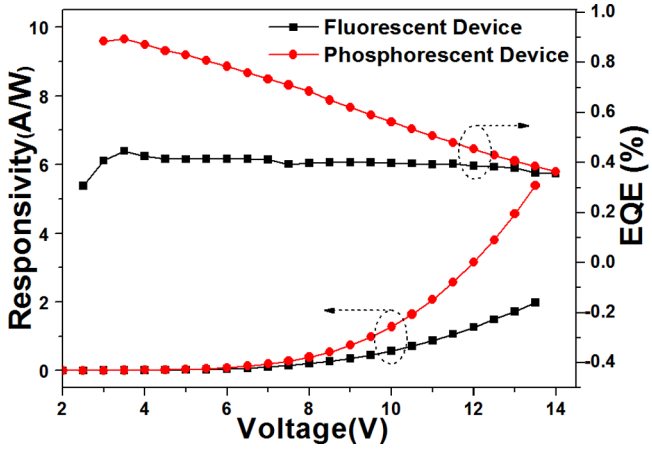

Figure 3. External quantum efficiency and responsivity of the upconverters under an IR illumination of 1 mW/mm^2 of the upconverters.

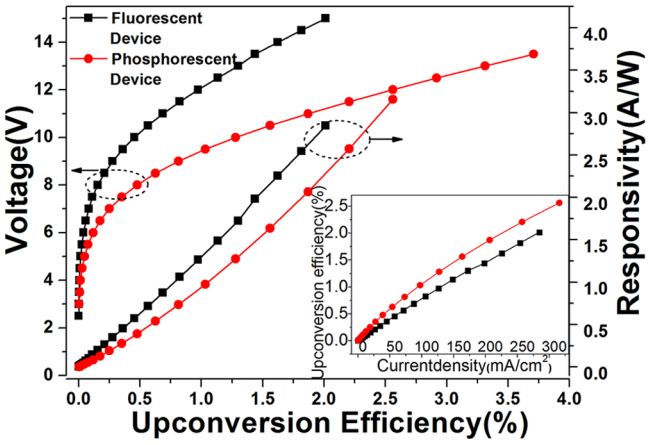

Figure 4. Voltage and responsivity of the upconverter at different upconversion efficiency. (inset) The current density dependence of the upconversion efficiency.

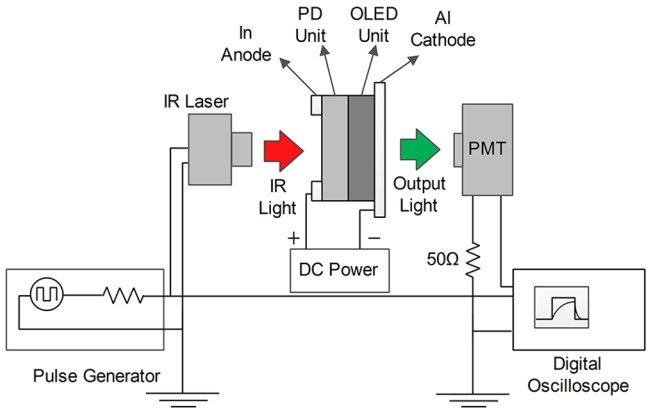

Figure 5. Experimental setup diagram for the upconverters transient response measurement.

As a comparison, the device using C545T:Alq_3 as EML was named as Fluorescent Device. When the upconverter was engaged in work, the PD unit was under reverse bias, and the OLED unit was under forward bias. The $In_{0.2}Ga_{0.8}As$/GaAs layer absorbed the inputted 980 nm near-infrared (NIR) light to generate photocarriers first. Then the photoinduced holes injected into organic layers through the OI interface. In emitting layer, the photoinduced holes combined with injected electrons. At last, the produced 510 nm green light emitted from the top semitransparent cathode. The PL spectrum curved in Figure 1b indicated that the PD unit had a responding range of 920−1000 nm. The absorption peak wavelength of the IR detection unit was located at 981 nm. Therefore, a 980 nm IR laser was adopted as excitation light source. When the upconverter was in working state, it outputted the green light with a wavelength of 510 nm. It clearly demonstrates that the optical upconversion process from IR to visible light can be achieved.

As is shown in Figure 2, the phosphorescent upconverter was irradiated under a 980 nm wavelength IR laser that switched on and off between adjacent voltages. Accordingly, the current density−voltage-luminance (J-V-L) performance shows a marked zigzag characteristic. When there was no NIR input (laser switch off), the current density and luminance were very low, like a dark state. However, they increased remarkably when the upconverter was under 1.0 mW/mm^2 NIR illumination. For instance, at the voltage of 12 V, the current density and output brightness were only 5.5 mA/cm^2 and 120 cd/m^2, respectively, with no NIR input. However, they jumped intensely to 320 mA/cm^2 and 4100 cd/m^2 when it was irradiated by 1.0 mW/mm^2 NIR. It can be implied that large number of photoinduced holes were generated in PD unit, and efficient injection to the adjacent OLED layers was achieved. In addition, the Phosphorescent Device can reach a maximum luminance of 7900 cd/m^2 at 15 V, much higher than that of 3700 cd/m^2 for Fluorescent Device.[30] It indicates that the hybrid device can convert 980 nm NIR to 510 nm visible light sensitively and efficiently.

Generally speaking, phosphorescent complex occupied a superior quantum efficiency to that of fluorescent materials in OLED. Therefore, the phosphorescent OLED can reach a higher brightness at relatively low power consumption compared to that of fluorescent device. On the basis of this point, $Ir(ppy)_3$:CBP was adopted as EML in the upconverter OLED unit to improve the total upconversion efficiency. As shown in Figure 3, external quantum efficiency (EQE) of the upconverter was calculated and compared. Attributing to the low light extraction efficiency of semitransparent Al cathode and poor hole injection from GaAs, we can see that the EQE of both Fluorescent Device and Phosphorescent Device were markedly lower than that of OLED based on indium tin oxide (ITO) substrate. However, despite the existence of efficiency roll-off phenomenon, the Phosphorescent Device still had a much higher EQE than that of the Fluorescent Device, especially when operated at low bias. For instance, at 5 V, an EQE of 0.84% can be achieved for the Phosphorescent Device, which was almost twice as much as that of Fluorescent Device (0.41%). Besides, the optical-electro conversion ability of the upconverter was described by photoresponsivity (A/W). The Phosphorescent Device also shows a superior responsivity than that of Fluorescent Device. At a low voltage of 12 V, the responsivity for Phosphorescent Device and Fluorescent Device was 1.3 A/W and 3.2 A/W, respectively. This indicates that phosphorescent complex is more efficient and suitable as EML for hybrid upconverter as the requirements of low power consumption.

To further investigate the power consumption at same upconversion efficiency, the working bias, current density, and responsivity of upconverters were compared in Figure 4. To achieve an upconversion efficiency of 2.0%, the Phosphorescent Device needed only a voltage of 11.2 V and a current density of 220 mA/cm^2. However, those quantities were 15 V and 280 mA/cm^2, respectively, for Fluorescent Device. The power consumption of the former one (24 mW) was 50% lower than the latter one. At 15 V, an upconversion efficiency of 4.8% can be achieved for Phosphorescent Device, much higher than that of the fluorescent device (2.0%). The upconversion efficiency exhibited almost a linear enhancement with the increase of responsivity. At a same responsivity and current density, which means a similar photocarrier injection, Phosphorescent Device can convert more inputted IR to green light. The markedly reduced energy consumption of Phosphorescent Device can be attributed to the higher quantum efficiency in its OLED unit.

The response speed must be taken into account if the OI hybrid upconverter could be applied to IR imaging device in the future. Therefore, we designed and set up a transient response test system to investigate the output luminance response of upconverter for the first time. As illustrated in Figure 5, the IR laser diode was driven by a fast rectangular

pulse generator with a rise time less than 20 ns. Then the IR pulse laser with an overall rise time less than 1 μs was obtained. The IR pulse was controlled with a width of 100 μs and a period of 30 ms. The generated green light pulse was detected by a high-speed photomultiplier tube (PMT). The resulting transient photocurrent was finally analyzed with a digital oscilloscope.

The transient luminance signal of Phosphorescent Device was displayed in Figure 6a. The intensity baseline of the

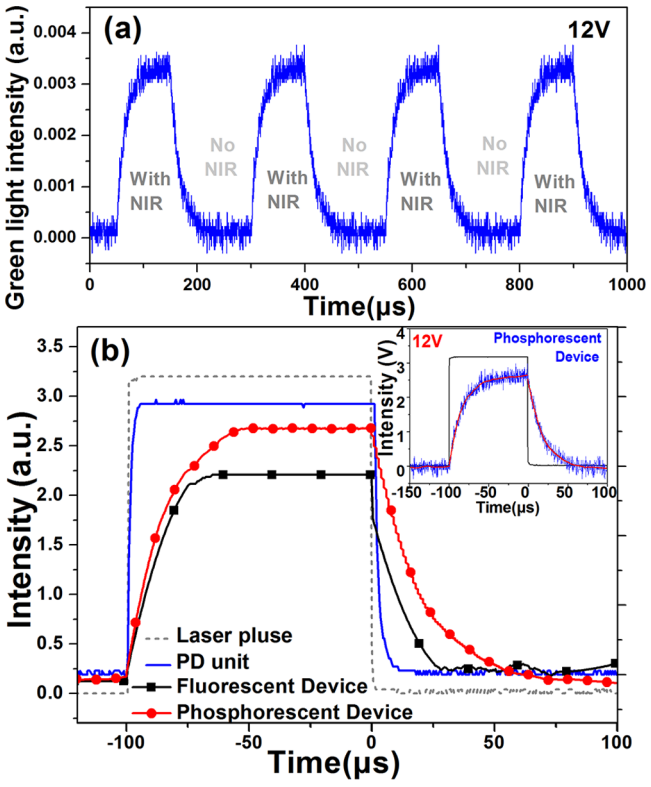

Figure 6. (a) The temporal response of outputted luminance under a square laser pulse irradiation in Phosphorescent Device. (b) Comparison of the fitted experimental response of PD unit, Fluorescent Device, and Phosphorescent Device in one single pulse. (inset) The response curve of Phosphorescent Device before and after fitting.

waveform represents the output luminance without NIR illumination, and the peak-to-peak level of the waveform shows the NIR pulse-excited luminance. Along with the applied IR pulse, the intensity of output green light rose immediately without delay and then reached to a steady value. Generally speaking, the rise (fall) time is defined as the time required to change the output green light response from 10% (90%) to 90% (10%) of its intensity.[35] It can be seen that the rise time and fall time is in the range of several tens of microseconds. The response curves of PD unit, Fluorescent Device, and Phosphorescent Device were fitted and compared in Figure 6b. They all worked at a bias of 12 V, and the inputted IR laser had a power density of 1.0 mW/mm^2. As is shown in Figure 6b, the IR laser and PD unit itself had a very fast rise times of less than 0.5 and 5 μs, respectively, which means their response would not be the test limits. The rise and fall times for Phosphorescent Device were 20 and 40 μs, respectively. The total response time of 60 μs can then be obtained by adding them together. We can see that the response time of Phosphorescent Device is slightly longer than that of Fluorescent Device. It can be attributed to the relatively long life of triplet exciton in phosphorescent materials. The interaction time between triplet excitons or between charges and triplet excitons would be prolonged as a result in EML.

To better understand the process of optical response, transient electric response under IR pulse irradiation was carried out and investigated. The upconverter was tandem connected with a resistance of 50 Ω. IR with a pulse width of 40 μs was irradiated from the back. Then the transient current was obtained by the detection of voltage changes on the resistance. As shown in Figure 7, the upconverter's electrical current

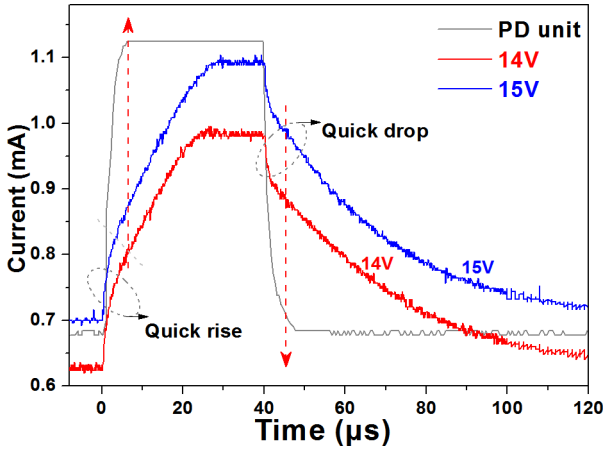

Figure 7. Transient electric response curves of the Phosphorescent Device under IR pulse irradiation. The solid gray line is the response curve of PD unit as a comparison.

response is similar to that of optical intensity. During the device operation, the PD unit was under reverse bias, and the OLED unit was under forward bias. Unlike the transient EL, the dark current injection balance from PD unit into OLED unit was built up even without IR pulse irradiation, as displayed in Figure 2. Therefore, both the transient current and the optical intensity increased immediately, or the delay time was very brief. When it comes to the transient electrical current, the two-step increases and drop phenomenon were more marked than that in optical response. When compared to PD unit, we can deduce that the two-step increase process was synchronized to the response of PD unit. As depicted in Figure 7, the transient current has an ~5 μs quick rise after the IR pulse switched on, and then it turned to a slow increase. The quick rise corresponds to the photoelectric response in PD unit at the first 5 μs, which generated large amounts of photocarriers. And then the slow increase was influenced by carrier injection between organic/inorganic heterojunction and carrier diffusion in OLED layers. The two-step decay process can be explained similarly.

Figure 8 displays the light response of Phosphorescent Device with different IR illumination density. They all worked at a bias of 15 V. We can see that they possessed similar waveforms except the outputted green light intensity and rise time. The higher the inputted IR intensity, the shorter the time needed to achieve saturated. For instance, as the power density of IR laser enhanced from 1.00 to 1.25 and to 1.50 mW/mm^2, the saturated time of outputted green light declined from 50 to 28 μs and then to 17 μs, respectively. Under a higher illumination level, more IR photos would be absorbed and

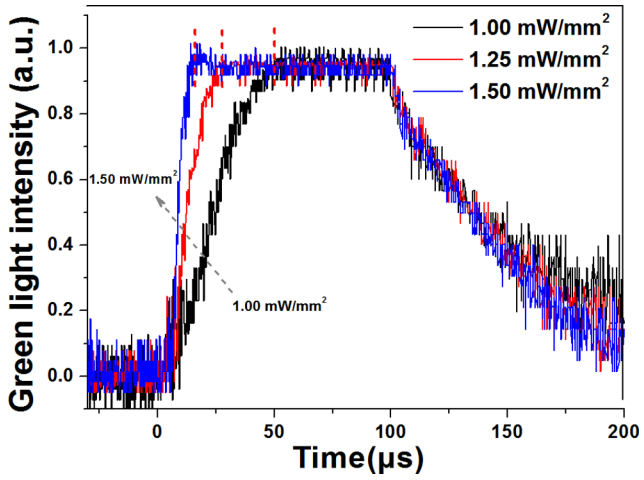

Figure 8. Normalized response curves of Phosphorescent Device under different IR irradiation.

more photocarriers would be generated in PD unit. As a result, the amounts of injected holes from GaAs to OLED unit would also increase. Therefore, the saturated time to achieve a same outputted light intensity was shortened.

To further explore other factors that affect response time, response characteristics of the Phosphorescent Device at different voltage were investigated, as is shown in Figure 9a.

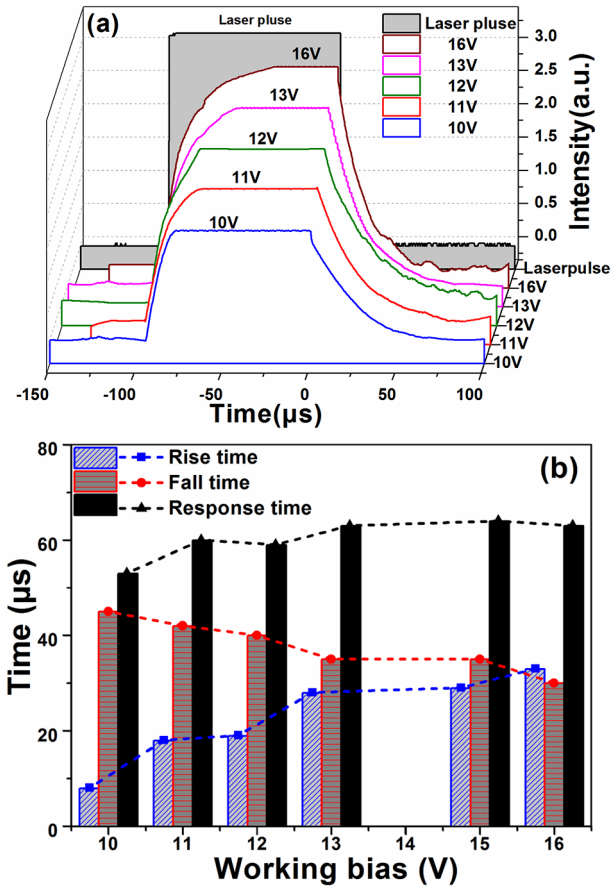

Figure 9. (a) The fitted response curves of Phosphorescent Device at different voltage. (b) Statistical analysis of rise time, fall time, and response time when the Phosphorescent Device worked at different biases.

Using a 1.0 mW/mm^2 IR pulse as excited step signal, the outputted green luminance rise and fall in an exponential pattern was also influenced by applied voltage significantly. As the bias increased from 10 to 16 V, the rise time has an increase from 9 to 33 μs, while the fall time decreased slightly from 45 to 30 μs, as revealed in Figure 9b. The overall response waveforms showed a feature that is similar to a first-order resistor−capacitor (RC) circuit. In hybrid upconverter, the diffusion capacitances of OLED increases along with bias, while the barrier capacitance of PD unit decreases with the increase of bias. Once they were tandem integrated, the overall resistance and capacitances both had a dependence on applied voltage. It is the same to the total RC constant of the upconverter. Therefore, we deduced it was the changes of total RC constant that determined variations in rise and fall times at different biases. The specific internal mechanism would be further explored in our subsequent studies. However, the overall response time just changed slightly from 50 to 60 μs. Accordingly, a high frequency of ∼20 kHz could be obtained if this hybrid upconverter is applied to IR imaging for 1 d. It would respond at least 50 times faster than the currently used LCD displays, whose response time ranged from 2 to 10 ms. Thus, the rapid response of this hybrid upconverter provides it a great application potential in high-speed IR imaging systems.

CONCLUSIONS

In conclusion, a hybrid optical upconverter based on an OLED and an inorganic photodetector has been fabricated and studied. It can convert irradiated 980 nm IR to 510 nm green light sensitively and successfully at room temperature. According to our results, the upconverter using phosphorescent OLED as display unit has a marked superiority compared to fluorescent one. It has been demonstrated that the former one can achieve higher conversion efficiency with relatively low power consumption. We also investigated the upconverter's optical and electic transient response properties for the first time. It has a response time of ∼60 μs, almost 50 times faster than that of the traditional LCD displays. IR intensity and applied voltage have been demonstrated to affect response time. The quick response of the upconverter provides a great application potential in high-speed IR imaging systems.

ASSOCIATED CONTENT

Supporting Information

Transient EL response of the phosphorescent device under electric pulse and the related testing system. This material is available free of charge via the Internet at http://pubs.acs.org.

AUTHOR INFORMATION

Corresponding Authors

*E-mail: guanmin@semi.ac.cn. (M.G.)
*E-mail: zhang_yang@mail.semi.ac.cn. (Z.Y.)

Notes

The authors declare no competing financial interest.

ACKNOWLEDGMENTS

The authors acknowledge the supports from National Natural Science Foundation of China (NNSFC 61274049, 61204012) and Beijing Natural Science Foundation (4132070, 4142053).

REFERENCES

(1) Abbas, M. M.; Kostiuk, T.; Ogilvie, K. W. Infrared Upconversion for Astronomical Applications. *Appl. Opt.* **1976**, *15*, 961−970.

(2) Tan, M. C.; Al-Baroudi, L.; Riman, R. E. Surfactant Effects on Efficiency Enhancement of Infrared-to-Visible Upconversion Emissions of $NaYF_4$: Yb-Er. *ACS Appl. Mater. Interfaces* **2011**, *3*, 3910−3915.

(3) Ring, E.; Ammer, K. Infrared Thermal Imaging in Medicine. *Physiol. Meas.* **2012**, *33*, R33.

(4) Hsieh, C.-C.; Wu, C.-Y.; Jih, F.-W.; Sun, T.-P. Focal-Plane-Arrays and CMOS Readout Techniques of Infrared Imaging Systems. *IEEE Trans. Circuits Syst. Video Technol.* **1997**, *7*, 594−605.

(5) Cohen, M. J.; Ettenberg, M. H.; Lange, M. J.; Olsen, G. H. Commercial and Industrial Applications of Indium Gallium Arsenide Near-Infrared Focal Plane Arrays. *Proc. SPIE* **1999**, 453−461.

(6) Challenor, M.; Gong, P.; Lorenser, D.; Fitzgerald, M.; Dunlop, S.; Sampson, D. D.; Swaminathan Iyer, K. Iron Oxide-Induced Thermal Effects on Solid-State Upconversion Emissions in $NaYF_4$: Yb, Er Nanocrystals. *ACS Appl. Mater. Interfaces* **2013**, *5*, 7875−7880.

(7) Zhao, L.; Peng, J.; Chen, M.; Liu, Y.; Yao, L.; Feng, W.; Li, F. Yolk−Shell Upconversion Nanocomposites for LRET Sensing of Cysteine/Homocysteine. *ACS Appl. Mater. Interfaces* **2014**, *6*, 11190−11197.

(8) Kruse, P.; Pribble, F.; Schulze, R. Solid State Infrared Wavelength Converter Employing High Quantum Efficiency Ge GaAs Heterojunction. *J. Appl. Phys.* **1967**, *38*, 1718−1720.

(9) Liu, Q.; Feng, W.; Yang, T.; Yi, T.; Li, F. Upconversion Luminescence Imaging of Cells and Small-Animals. *Nat. Protoc.* **2013**, *8*, 2033−2044.

(10) Hiramoto, M.; Yoshimura, K.; Miyao, T.; Yokoyama, M. Up-Conversion of Red Light to Green by a New Type of Light Transducer using Organic Electroluminescent Diode Combined with Photoresponsive Amorphous Silicon Carbide. *Appl. Phys. Lett.* **1991**, *58*, 1146−1148.

(11) Luo, H.; Ban, D.; Liu, H.; SpringThorpe, A.; Wasilewski, Z.; Buchanan, M.; Glew, R. 1.5 to 0.87 μm Optical Upconversion using Wafer Fusion Technology. *J. Vac. Sci. Technol.* **2004**, *22*, 788−791.

(12) Luo, H.; Ban, D.; Liu, H.; Poole, P.; Buchanan, M. Pixelless Imaging Device Using Optical Up-Converter. *IEEE Electron Device Lett.* **2004**, *25*, 129−131.

(13) Liu, H. C.; Gao, M.; Poole, P. 1.5 μm Up-Conversion Device. *Electron. Lett.* **2000**, *36*, 1300−1301.

(14) Kim, D. Y.; Song, D. W.; Chopra, N.; De Somer, P.; So, F. Organic Infrared Upconversion Device. *Adv. Mater.* **2010**, *22*, 2260−2263.

(15) Kim, D. Y.; Choudhury, K. R.; Lee, J. W.; Song, D. W.; Sarasqueta, G.; So, F. PbSe Nanocrystal-Based Infrared-to-Visible Up-Conversion Device. *Nano Lett.* **2011**, *11*, 2109−2113.

(16) Chikamatsu, M.; Ichino, Y.; Takada, N.; Yoshida, M.; Kamata, T.; Yase, K. Light Up-Conversion from Near-Infrared to Blue using a Photoresponsive Organic Light-Emitting Device. *Appl. Phys. Lett.* **2002**, *81*, 769−771.

(17) Guan, M.; Li, L.; Cao, G.; Zhang, Y.; Wang, B.; Chu, X.; Zhu, Z.; Zeng, Y. Organic Light-Emitting Diodes with Integrated Inorganic Photo Detector for Near-Infrared Optical Up-Conversion. *Org. Electron.* **2011**, *12*, 2090−2094.

(18) Chen, J.; Ban, D.; Helander, M. G.; Lu, Z.-H.; Poole, P. Near-Infrared Inorganic/Organic Optical Upconverter with an External Power Efficiency of >100%. *Adv. Mater.* **2010**, *22*, 4900−4904.

(19) Chen, J.; Ban, D.; Helander, M. G.; Lu, Z.; Graf, M.; SpringThorpe, A. J.; Liu, H. C. Near-Infrared Optical Upconverter Based On i-$In_{0.53}Ga_{0.47}As/C_{60}$ Photovoltaic Heterojunction. *Electron. Lett.* **2009**, *45*, 753−755.

(20) Chen, J.; Ban, D.; Feng, X.; Lu, Z.; Fathololoumi, S.; SpringThorpe, A. J.; Liu, H. C. Enhanced Efficiency in Near-Infrared Inorganic/Organic Hybrid Optical Upconverter with an Embedded Mirror. *J. Appl. Phys.* **2008**, *103*, 103112.

(21) Ban, D.; Han, S.; Lu, Z. H.; Oogarah, T.; SpringThorpe, A. J.; Liu, H. C. Near-Infrared to Visible Light Optical Upconversion by Direct Tandem Integration of Organic Light-Emitting Diode and Inorganic Photodetector. *Appl. Phys. Lett.* **2007**, *90*, 093108.

(22) Matyba, P.; Yamaguchi, H.; Eda, G.; Chhowalla, M.; Edman, L.; Robinson, N. D. Graphene and Mobile Ions: The Key to All-Plastic, Solution-Processed Light-Emitting Devices. *ACS Nano* **2010**, *4*, 637−642.

(23) Forrest, S. R. The Path to Ubiquitous and Low-Cost Organic Electronic Appliances on Plastic. *Nature* **2004**, *428*, 911−918.

(24) Shu, T.; Wu, J.; Lu, M.; Chen, L.; Yi, T.; Li, F.; Huang, C. Tunable Red−Green−Blue Fluorescent Organogels on the Basis of Intermolecular Energy Transfer. *J. Mater. Chem.* **2008**, *18*, 886−893.

(25) Yun, W. M.; Jang, J.; Nam, S.; Kim, L.; Seo, S. J.; Park, C. E. Thermally Evaporated SiO Thin Films as a Versatile Interlayer for Plasma-Based OLED Passivation. *ACS Appl. Mater. Interfaces* **2012**, *4*, 3247−3253.

(26) Pudasaini, P. R.; Ruiz-Zepeda, F.; Sharma, M.; Elam, D.; Ponce, A.; Ayon, A. A. High Efficiency Hybrid Silicon Nanopillar−Polymer Solar Cells. *ACS Appl. Mater. Interfaces* **2013**, *5*, 9620−9627.

(27) Heliotis, G.; Itskos, G.; Murray, R.; Dawson, M. D.; Watson, I. M.; Bradley, D. D. C. Hybrid Inorganic/Organic Semiconductor Heterostructures with Efficient Non-Radiative Energy Transfer. *Adv. Mater.* **2006**, *18*, 334−338.

(28) Liu, D.; Zhao, M.; Li, Y.; Bian, Z.; Zhang, L.; Shang, Y.; Xia, X.; Zhang, S.; Yun, D.; Liu, Z.; Cao, A.; Huang, C. Solid-State, Polymer-Based Fiber Solar Cells with Carbon Nanotube Electrodes. *ACS Nano* **2012**, *6*, 11027−11034.

(29) Bolink, H. J.; Brine, H.; Coronado, E.; Sessolo, M. Ionically Assisted Charge Injection in Hybrid Organic− Inorganic Light-Emitting Diodes. *ACS Appl. Mater. Interfaces* **2010**, *2*, 2694−2698.

(30) Chu, X. B.; Guan, M.; Li, L. S.; Zhang, Y.; Zhang, F.; Li, Y. Y.; Zhu, Z. P.; Wang, B. Q.; Zeng, Y. P. Improved Efficiency of Organic/Inorganic Hybrid Near-Infrared Light Upconverter by Device Optimization. *ACS Appl. Mater. Interfaces* **2012**, *4*, 4976−4980.

(31) Chu, X. B.; Guan, M.; Zhang, Y.; Li, Y. Y.; Liu, X. F.; Zhu, Z. P.; Wang, B. Q.; Zeng, Y. P. Influences of Organic-Inorganic Interfacial Properties on the Performance of a Hybrid Near-Infrared Optical Upconverter. *RSC Adv.* **2013**, *3*, 23503−23507.

(32) Kishore, V.; Patankar, M. P.; Periasamy, N.; Narasimhan, K. L. Transient Electroluminesence in Alloy-Based Organic Light-Emitting Diodes. *Synth. Met.* **2004**, *143*, 295−303.

(33) Rui, L.; Zhengqing, G.; Shinar, R.; Shinar, J. Transient Electroluminescence Spikes in Small Molecular Organic Light-Emitting Diodes. *Phys. Rev. B* **2011**, *83*, 245302.

(34) Hassine, L.; Bouchriha, H.; Roussel, J.; Fave, J. L. Transient Response of a Bilayer Organic Electroluminescent Diode: Experimental and Theoretical Study of Electroluminescence Onset. *Appl. Phys. Lett.* **2001**, *78*, 1053−1055.

(35) Morimune, T.; Kajii, H.; Ohmori, Y. Photoresponse Properties of a High-Speed Organic Photodetector based on Copper−Phthalocyanine under Red Light Illumination. *IEEE Photonics Technol. Lett.* **2006**, *18*, 2662−2664.